



3rd Trondheim Gas Technology Conference, TGTC-3

## Investigation of non-ideal behavior of plate-fin heat exchangers in LNG services

G. Skaugen<sup>a,\*</sup>, M. Hammer<sup>a</sup>, M. Aa. Gjennestad<sup>a</sup>

<sup>a</sup>SINTEF Energy Research  
N-7465 TRONDHEIM  
Norway

---

### Abstract

Using a heat exchanger with several parallel channels in boiling services, static instabilities like the Ledinegg instabilities can occur, resulting from a combination of unfortunate operating conditions and the heat exchanger design. Ledinegg instability is characterized by different flow rates in parallel channels that share common inlet and outlet manifolds. Oscillations between different conditions may also occur. In a thermodynamic system like liquefaction of natural gas, the fluids can exhibit a large temperature glide during condensation and evaporation and the actual local fluid temperature inside a heat exchanger will then be directly dependent of the local mass-flow. This means that mass-flow oscillations also imply thermal oscillations. This study shows how this type of non-ideal behavior can be predicted for a plate-fin heat exchanger by requiring all channels for each stream to have equal pressure drop. These nonlinear equations are solved on top of the thermo-hydraulic simulation model for the heat exchanger core.

© 2015 Published by Elsevier Ltd. This is an open access article under the CC BY-NC-ND license (<http://creativecommons.org/licenses/by-nc-nd/4.0/>).

Peer-review under responsibility of the Scientific Committee of TGTC-3

**Keywords:** LNG, Process modelling, Heat exchanger design, Plate-fin, instability

---

### 1. Introduction

With a growing focus on offshore natural gas (NG) liquefaction and processing, efficient processes and compact equipment with lower weight and smaller footprint are of vital importance. In processes for the cooling, condensation and sub-cooling of natural gas from ambient temperatures to around  $-160^{\circ}\text{C}$ , the main cryogenic heat exchanger is one of the most cost- and energy-intensive process component. NG liquefaction processes are frequent subjects of optimisation studies in the literature, but seldom take into account geometrical effects and operational constraints of the heat exchangers. The most common approach is to do thermodynamic optimization, in which the details of the heat exchanger are not resolved. From the thermodynamic optimal process conditions, heat exchangers are designed independently given only a duty requirement and a maximum allowable pressure drop. A recent example is the optimization of the propane pre-cooled mixed-refrigerant (C3MR) process presented by Wang et al. [18]. Here, all the hot streams in the

---

\*Corresponding author

Email address: [geir.skaugen@sintef.no](mailto:geir.skaugen@sintef.no) (G. Skaugen)

main heat exchanger were combined to form a single hot composite curve which exchanged heat with the cold stream, specifying 2 K in the Minimum Internal Temperature Approach (MITA) as a constraint for the optimization. The required heat transfer rates (UA-values) were calculated based on the overall heat balance between the hot and cold streams. Pressure drops in the heat exchanger were set to zero. In the actual optimization, the refrigerant composition was fixed and the remaining free variables were the two pressure levels and the refrigerant flow rate. A limitation of using only MITA as a constraint for the heat exchanger, is that it does not constrain its size. The optimization will try to obtain a solution in which the overall temperature difference is equal to MITA. This may be neither feasible nor necessarily the optimum solution. Consequences of using a single hot composite stream rather than specifying individual warm streams were discussed by Chang et al. [5]. In their thermodynamic optimization, they used individual UA-values for each warm stream as parameters and established an optimum ratio between them. They concluded that the temperature profile with the MITA formulation was very difficult to realize in a practical multi-stream heat exchanger, and that the figure of merit for the process, defined as the ratio between theoretical minimum work and actual work, was overestimated. The liquefaction capacity or size of the heat exchanger was not part of the study.

A stand-alone optimization of plate fin heat exchanger geometry for specific process streams was described by Reneaume and Niclout [13, 14], whose work included detailed models for heat transfer, pressure drop and thermo-physical properties and also handled phase changes. They achieved 15 to 21% reductions in manufacturing costs by utilising a defined available pressure drop for each stream and optimizing several geometrical parameters. In their model, the authors combined the warm and cold streams into composite streams and used a common wall temperature approach and used constant values for the thermo-physical properties such as dynamic viscosity, thermal conductivity and specific heat capacity for each stream.

The aim of the modelling framework presented in this work, is to geometrically describe a heat exchanger and include this as a unit model in a process simulation environment, so that a combined operational and heat exchanger design optimization can be performed.

## 2. Flexible heat exchanger modeling framework

A robust and flexible modelling environment suitable for multi-stream heat exchangers was used in this work. This modelling framework itself is described in more detail by Skaugen et al. [17]. It can be used to model and analyze the performance of almost any type of heat exchanger. Rather simple heat exchanger elements that consist of a fluid node and an array of surfaces must be defined, where each surface can have a detailed geometric description. The heat exchanger elements are linked in the sequence of the fluid streams and each surface are coupled to a solid wall temperature node. Thus, the full geometry and the flow-circuiting of a heat exchanger can be described numerically. Once a heat exchanger has been described, the model can be parameterized using any number of underlying geometry details.

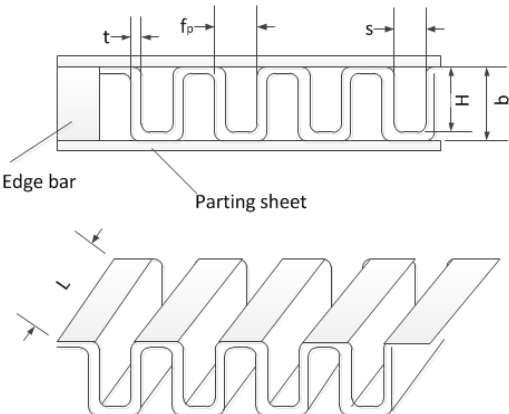
Local convective heat fluxes are calculated when the performance of each stream when the evolution of the specific enthalpy and pressure is integrated from the inlet. The fluid of each stream is described using the one-dimensional steady-state Euler equations with source terms for friction, gravity and heat transfer. The one-dimensional equations represent the area-averaged, plug-flow formulation of the general three dimensional conservation equations. The local heat flux over a surface is based on the temperature difference between the bulk stream temperature and the specific surface temperature and the local heat transfer coefficient. The surface temperatures are later updated by solving a set of non-linear algebraic equations for the solid temperatures by means of a slightly modified DNSQE routine from the SLATEC library [7]. The heat balance equations include conductive heat transfer in addition to the convective fluxes, so effects of longitudinal heat conduction are automatically included. The heat exchanger is solved when the net heat flux around each solid temperature node is zero.

### 2.1. Plate-fin heat exchanger model description

A plate-fin heat exchanger (PFHE) was implemented as a multi-layer, multi-stream heat exchanger model. It is defined by first creating a number of possible channel geometries using the fin parameters

shown in Table 1. Next, the created geometries are assigned to various layers and finally, streams are assigned to each of the defined layers. For each fin geometry, the surface perimeter and the channel cross sectional area defines the hydraulic diameter,  $D_h$ , that is used by the underlying models for calculating heat transfer and pressure drop.

Table 1: Geometry parameters required to describe a PFHE channel



Fin type: Plain, Perforated or Serrated		Fin distance or passage width (m):	$s = f_p - t$
Fin thickness (m):	$t$	Parting sheet distance (m):	$b = H + t$
Fin pitch (m):	$f_p = 1/\text{frequency}$	Parting sheet thickness (m):	$p_t$
Fin height or passage height (m):	$H$	Perforation factor (-):	$p$
Fin length or serration length (m):	$L$	Edge bar thickness (m):	$t_e$
		Layer width (m)	$W$

Fin specific heat transfer and pressure drop correlations are used in the model. They are expressed as a Nu-number or a  $j$ -factor correlation for heat transfer and an  $f$ -factor correlation for the wall friction. These are used for the single phase region. The Nu-number and the Colburn  $j$ -factor relates to the heat transfer coefficient,  $\alpha$ , as:  $Nu = \frac{\alpha D_h}{\lambda}$  and  $j = \frac{Nu}{Re Pr^{1/3}}$ . The Prandtl number is defined as:  $Pr = \frac{\mu C_p}{\lambda}$  where  $\lambda$  is the thermal conductivity,  $\mu$  the dynamic viscosity and  $C_p$  is the specific heat capacity.

In the implemented model, the heat transfer coefficient for rectangular plain fins is calculated with the correlation from Gnielinski [9] and the friction factor from Filonenko [6]. For serrated fins, a  $j$ -factor and an  $f$ -factor correlation from Manglik and Bergels [12] are used. Perforated fins are treated as plain fins, but with the surface multiplied with the perforation factor,  $p$ , (usually about 0.95, meaning that 5% of the area are lost due to perforation) and the friction factor is increased by 20% as recommended by Hesselgreaves [10].

In two-phase regions, the pressure drop is calculated from the correlation by Friedel [8] while for heat transfer, the correlation by Bennett and Chen [3] is used for boiling and the correlation from Boyko and Kruzhilin [4] is used for condensation. Both boiling and condensation heat transfer coefficients are moderated according to the methods of Silver [15] and Bell and Ghaly [2] due to the large temperature glide of both the natural gas and the refrigerant mixture.

## 2.2. PFHE model - layer and stream configuration

The different streams in the PFHE are flowing in individual layers where each layer consists of several channels. This is illustrated in Figure 1a where three layers A, B and C each consists of multiple channels with individual geometries I, II and III.

When the complete heat exchanger model is generated, it can be done by connecting each individual channel to their own surface or by lumping all channels in the layer together and connect these to one common surface. The difference between a “lumped” layer-by-layer model and a full individual layer-by-layer models will be demonstrated later. Note that for a lumped model, the cross sectional wall temperatures at given (axial) position will be different for the different layers but will be equal within each layer.

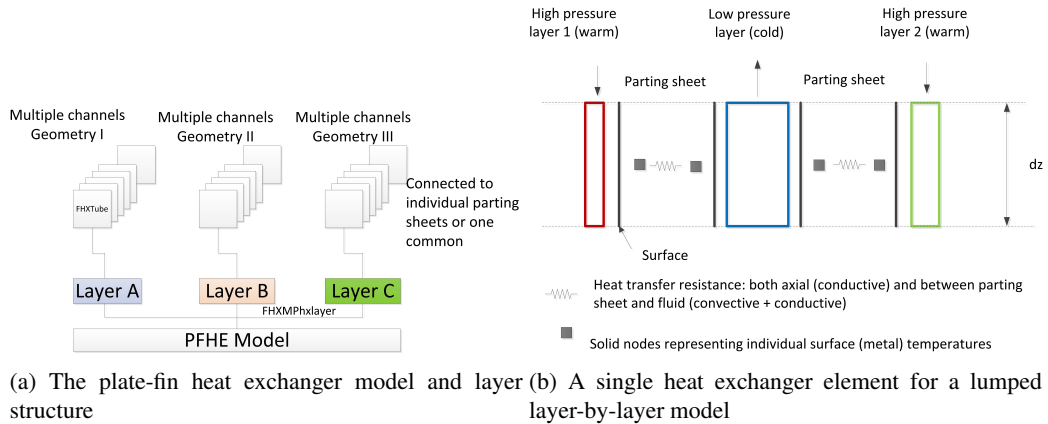


Fig. 1: Illustration of the PFHE model with layers, streams and element

In the final model, using lumped or individual channel definition, each heat exchanger element has a “right” and a “left” surface. Each surface in the heat exchanger element points to a solid node that holds the actual wall temperature. Each solid node in the model has two “ports” that can be linked either to a heat-transfer resistance element or to a surface element. The illustration of one heat exchanger element for each of the three streams are shown for a lumped layer-by-layer model in Figure 1b. Here the element for the natural gas (green) is connected to one surface. This surface is coupled to a solid node representing the actual wall temperature. The MRLP element (blue) is linked to two surfaces, facing each of the warm streams (NG and MRHP). The two thermal resistors provide the temperature difference through the walls.

The implemented model was validated against the Aspen MUSE from Aspen Technology, Inc [1] run in MULE- (layer-by-layer) mode. Aspen MUSE has a very good reputation among PFHE manufacturers and it is considered to be an industry reference model. The case for validation is liquefaction of natural gas using a single mixed refrigerant (SMR) process. The process and the heat exchanger data for the natural gas (NG), the high pressure mixed refrigerant (MRHP) and the low pressure mixed refrigerant (MRLP) streams are shown in Table 2. The results from the comparison are shown in Figures 2 and 3.

Table 2: Geometry and operating conditions used for validation of the PFHE-model with MUSE.

Number of parallel blocks	12		
Width (mm) × Depth (mm) × Active length (mm)	1173 × 1272 × 5150		
	MRLP	MRHP	NG
Number of layers	1416	720	180
Fin type	Perforated	Serrated	Serrated
Fin height (mm)	5.1	5.1	5.1
Fin thickness (mm)	0.3	0.3	0.4
Fin frequency ( $m^{-1}$ )	787	787	787
Parting sheet thickness (mm)	2.0	2.0	2.0
Inlet temperature (K)	116.05	298.15	298.5
Inlet pressure (bar)	5.34	25.88	55.0
Inlet vapor fraction (-)	0.032	0.67	1.0
Mass flow rate ( $kg s^{-1}$ )	101.0	101.0	17.7
Mass flux ( $kg m^{-2} s^{-1}$ )	19.48	33.57	26.76
Flow direction	Up	Down	Down

In Figure 2a, the estimated capacity from the two models is compared. As seen, the discrepancy between the models is very small. The reason is that the approach temperature in both cold and warm end is quite close and quite small. In Figure 2b, showing the stream pressure drops, the discrepancies are larger. One

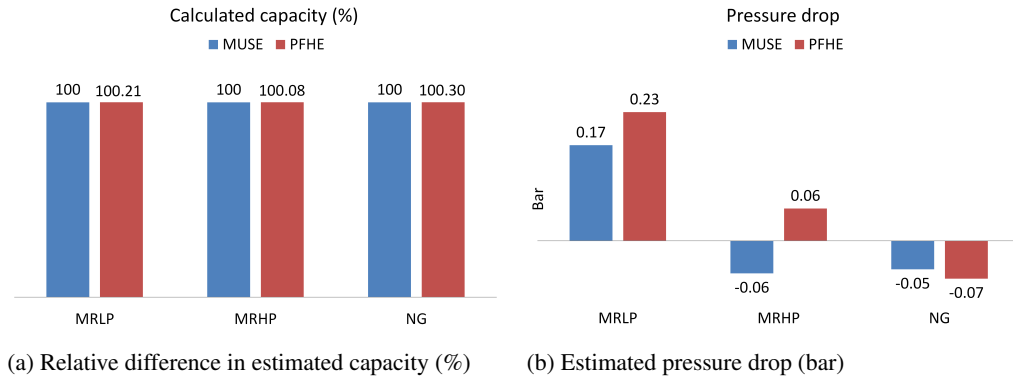


Fig. 2: Comparing calculated capacity and pressure drop between the PFHE model with Aspen MUSE in layer-by-layer mode

reason is that the implemented PFHE model does not include a sophisticated distributor pressure drop model. The pressure drops in the three streams are quite moderate for the investigated case. In Figures 3a and 3b, comparison of local conditions are shown. The temperature profiles in Figure 3a show quite similar behavior for the two models and the transitions between the various single phase and two-phase regions for all streams are also similar as shown by the evolution of the vapor fraction in Figure 3b. The graphs show that the developed PFHE model takes into account the local thermo-hydraulic effects at that it can be used for further studies to gain insight in the behavior of PFHE's under different operating conditions and geometrical configuration.

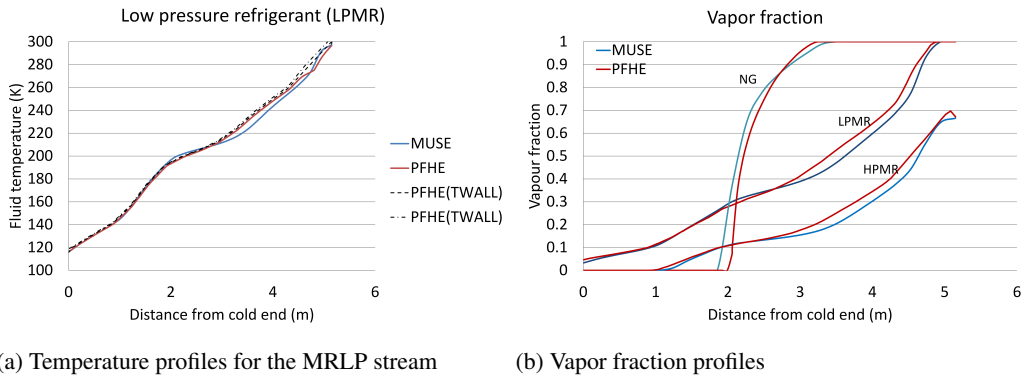


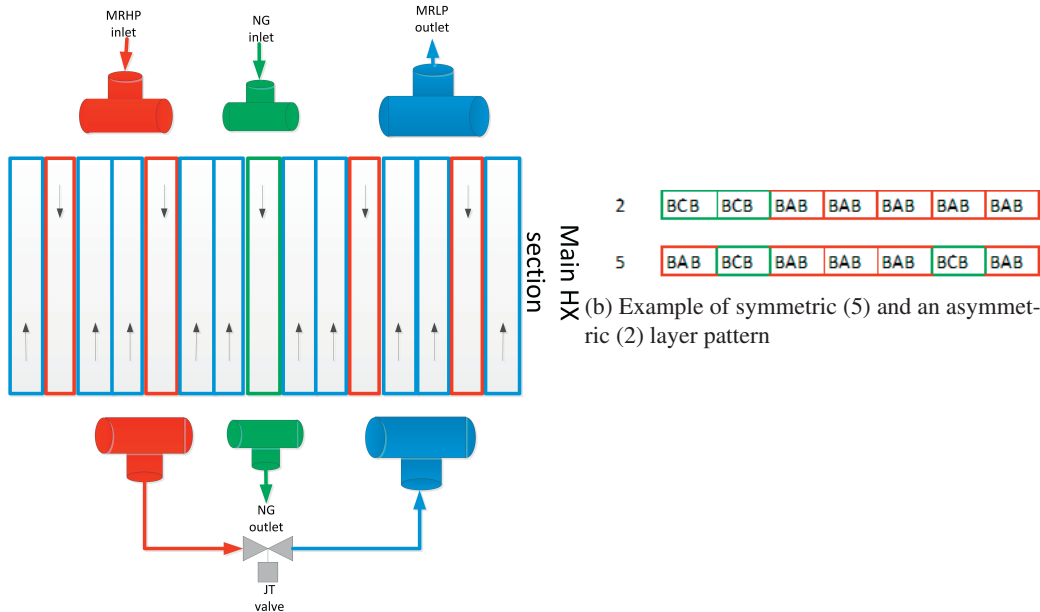
Fig. 3: Comparing temperature and vapor fraction profile between the lumped PFHE model and Aspen MUSE

### 2.3. Modelling of individual layers

As described in Section 2.2, individual channels can be linked through individual walls or lumped together in larger sections. The solution algorithm for the model is to find the wall temperatures that will ensure a zero net heat flux around each temperature node. This means that the number of variables that need to be solved will increase radically when the model is configured to solve for each individual channel.

The PFHE model is also configured to include a Joule-Thompson (J/T)-valve between the outlet of the high pressure and inlet of the low pressure refrigerant layers. This is done by including manifold elements in the model that will collect and distribute the flow between individual layers. The valve element is connected between two manifolds. The manifold element and valve element are linked together with the normal heat exchanger elements with when a full circuit is defined. These elements are slightly different and contain no

surfaces. In Figure 4a a part of the complete heat exchanger is shown, including one layer for the NG, four layers for the MRHP- and ten layers for the MRLP-stream.



(a) A PFHE model with the integrated Joule-Thomson valve

Fig. 4: Illustration of a layer-by-layer model and examples of specification of layer patterns

When evaluating effects of flow mal-distribution an additional set of equations is added to the system. They are solved using the individual channel flow rates as free variables  $\dot{m}_{ij}$ . Here,  $i$  is the stream index and  $j$  is the layer (or channel) index. All the channel flows must be positive,

$$\dot{m}_{ij} > 0, i \in \{1, ns\}, \quad \forall j \in [2, nl_i]. \quad (1)$$

where  $ns$  is the number of streams and  $nl_i$  is the number of layers in stream  $i$ . The overall number of variables become,  $n = \sum_{i=1}^{ns} nl_i$ .

The pressure drop over each channel for all the three streams shall be equal, and the sum of the individual flow rates in each channel in a layer shall be equal to the specified total flow rate for the NG, the MRHP and the MRLP stream. In the examples above, in Figure 4a, there are a total of 20 equations that have to be solved. In the function evaluations, the heat exchanger has to be solved thermally, which means that all metal temperatures need to be found. To speed up the calculation, the solution for the metal temperatures are stored and used as initial values between each function evaluation. The inclusion of the JT-valve ensures that the inlet specific enthalpy to the MRLP stream is equal to the outlet specific enthalpy of the MRHP stream, eliminating one possible extra system level equation.

The equations for equal pressure drop for each stream are:

$$\Delta p_{i,j}(\dot{\mathbf{m}}) - \Delta p_{i,1}(\dot{\mathbf{m}}) = 0, \quad \forall i \in [1, ns], j \in [2, nl_i]. \quad (2)$$

Overall there are  $n - ns$  number of pressure drop equations.

The equations for the flow rates are

$$\sum_{j=1}^{nl_i} \dot{m}_j - \dot{m}_i = 0, \quad \forall i \in [1, ns]. \quad (3)$$

Overall there are *ns* number of flow rate equations.

The set of non-linear (2) and linear (3) equations are solved using the gradient-based solver DNSQE from the SLATEC library.

### 3. Results from the simulation

With a two-dimensional layer-by-layer model, effects like flow mal-distribution, geometry imperfections or different stacking pattern can be investigated. In the examples below, the PFHE model has been used to study the differences between using a layer-by-layer and a lumped model formulation, by using two different stacking patterns and to investigate the possibilities of multiple solution when static instability may occur.

#### 3.1. Effects from different stacking pattern

Effects of mal-distribution occurring from using different stacking-patterns are studied below. As test case,  $\frac{1}{20}$  of a full heat exchanger is studied, having two layers for the natural gas (C), five layers for the high pressure refrigerant (A) and 14 layers for the low pressure refrigerant (B). In Figure 4b a symmetric and an asymmetric pattern are shown. In the illustration, layers are grouped in three for clarity, with the three-layer group containing the natural gas layer shown in green color. Here, layer pattern 2 will have a quite asymmetric heat load, placing the natural gas layer to one side. In layer pattern 5, the natural gas layers are more evenly distributed across the flow area with asymmetric load occurring only from end channel effects.

The effect on the flow distribution is shown in Figure 5. In Figure 5a, the symmetric layer configuration, the maximum flow mal-distribution of the low pressure refrigerant stream is about 5% and showing no maldistribution for the NG-stream, while in Figure 5b, the flow mal-distribution of the MRLP stream varies between -18% to 12%. The effects on the MRHP and NG-stream are still moderate with about 1% and 0.5% mal-distribution. Next, the implication on the sizing of the heat exchanger is demonstrated. The lumped

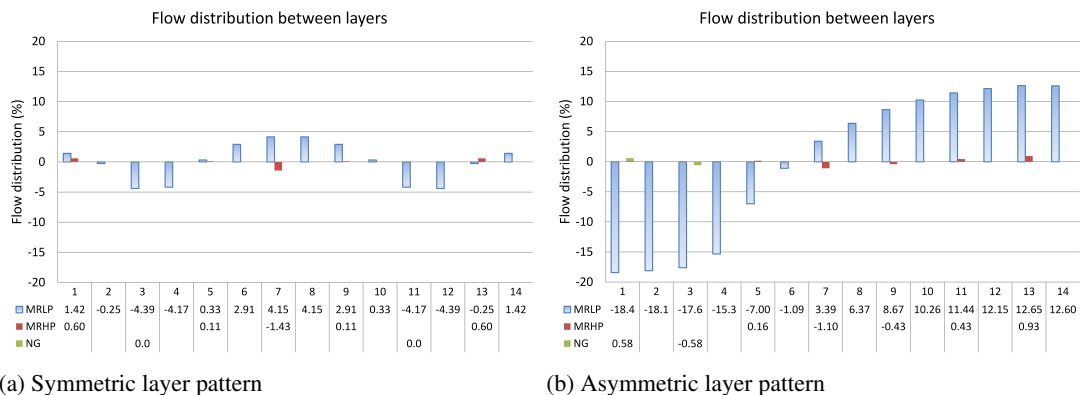


Fig. 5: Flow distribution between layers for a symmetric (5) and asymmetric (2) layer pattern

layer model is used as the reference. In the layer-by-layer configuration two sets of simulations are run, one with the same geometry as the reference case and a second where the active length, (*L*), is added as a free geometry variable. One additional equality constraint is then required and is shown in Eq. (4). This will ensure that the mixed outlet natural gas temperature from the two NG layers are equal to the outlet natural gas temperature from the reference case.

$$T_{NG,out}(L) - T_{NG,out,ref}(L_{ref}) = 0. \tag{4}$$

The mixed NG outlet temperature is calculated by performing an enthalpy-pressure flash, where the mixture specific enthalpy are used as the input specification. The outlet pressure from each layer for a stream is equal. When the solution is found, the additional length compared to the reference case is reported as “required oversizing” in Table 3.

As seen, even if the effects on the capacity seem insignificant with less than 2% loss of performance in the asymmetric case, it will have a more significant effect on the resulting mixture outlet NG temperature and on the required oversizing. This is due to the (already) very small temperature differences between the warm and the cold streams. As an alternative to the oversizing, the process can operate with a lower suction pressure which will require more compressor power. This is not evaluated in the stand-alone heat exchanger model, but can be included if the heat exchanger model is included as a unit model in a process simulation environment. In Figure 6, the wall temperature profiles (a) and the stream vapor fraction profiles

Table 3: Main results from the simulations

	Lumped layer model	Symmetric	Asymmetric
Cooling capacity (kW)	1750	1731 (-1.03%)	1718 (-1.81%)
Outlet NG temp. (K)	116.6	118.9 (+2.3)	121.2 (+4.6)
Required oversizing		22%	38%

(b) for all layers are shown. The red curves are the reference case using the lumped model and show one wall temperature profile and one vapor fraction profile for each stream. Using the layer-by-layer model shows how the asymmetry effects move the warm section of the heat exchanger toward the J/T-valve. In the reference case, about 35% of the heat exchanger length is required to get the NG fully condensed, for the symmetric layer configuration 40% is required and for the asymmetric case, 60% is required. These differences will also have impact on the outlet MRHP temperature. Since the J/T-valve is integrated in the heat exchanger model, a higher outlet MRHP temperature will also affect the inlet temperature for the MRLP and thus reduce the cooling capacity.

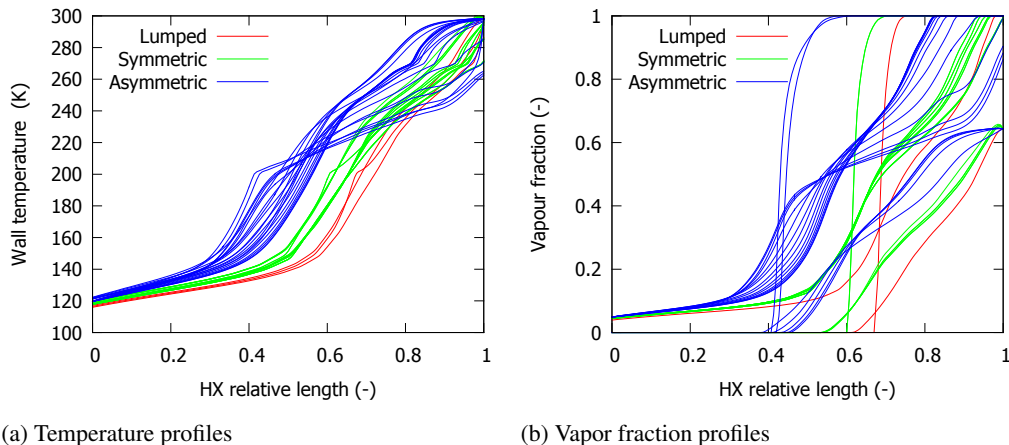


Fig. 6: Temperature and vapor fraction profiles for the reference layer-by-layer model (red), symmetric (green) and asymmetric (blue) layer pattern

### 3.2. Ledinegg instability

In Skaugen et al. [16] the possibilities of static instability occurring in plate-fin heat exchangers were thoroughly discussed. The investigated heat exchanger design in this work also show possibilities of Ledinegg instability occurring [11]. Using the lumped layer model to vary the low pressure refrigerant flow rate around the design flow rate, the N-shaped curve for the flow-rate vs. pressure drop occurs as shown in Figure 7a. The design point flow rate is located on the negative slope on the N-shape and this is an indication that a mal-distribution solution may exist, simply from the hypothesis that if the total flow rate can pass through the heat exchanger with a lower pressure drop than the pressure drop calculated at the design point, it will. This means that some channels will operate with higher mass flux and some channels with



lower mass flux than the average design value. This also means that some parts of the heat exchanger may have super-heated refrigerant outlet, while other parts will have liquid surplus at the outlet. After mixing, the average outlet condition can be in the two-phase region, requiring some sort of stream recycling from the refrigerant compressor to boil off any liquid surplus.

In the following analysis only the pressure drop through the active heat transfer area was evaluated and the symmetric stacking pattern was used. This problem has at least two solutions for the refrigerant flow distribution, and which of the solutions that are found, depend on the initial values of the refrigerant flow-rate within each individual layer. In Figure 7b, two sets of wall temperature profiles are shown, both being a solution of the problem, meaning the pressure drop through each individual channel are equal, but the total pressure drop for the two solutions are different. The set with the green curves shows the solution where there is practically no mal-distribution of the refrigerant flow. The red curves are the solution occurring when the initial refrigerant flow-rate is mal-distributed. The full “spread” of wall temperature is the result of the strong thermal coupling between the individual layers through the partition sheet. An analysis of breaking

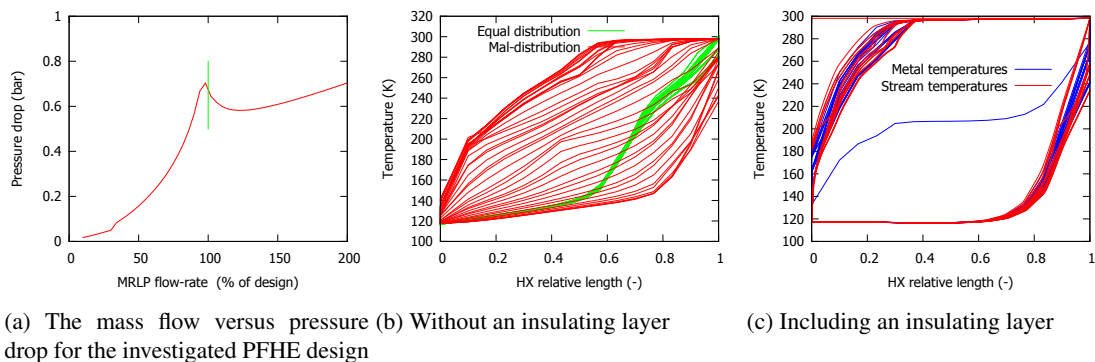


Fig. 7: The wall temperature profiles between each layer of the investigated PFHE with full mass flow distribution

the thermal coupling was also done and is shown in Figure 7b. Here an insulating dummy layer D was added in the center of the stacking pattern 2 from Figure 4b. No heat is transferred across this layer. Then, with mal-distributed initial flow rate for the low pressure refrigerant, the situation shown in Figure 7c occurs. The heat exchanger will have a warm section where all the heat is transferred in the first part and a cold section where all the heat is transferred in the last part of the heat exchanger. The metal temperature in the middle is the temperature on the insulated layer in the model. In a practical heat exchanger a manufacturing defect could also break the thermal coupling and produce similar results. Also in this case, with initial equal distribution of the flow, the solution is a “nice” temperature profile as the green profile in Figure 7b.

The conclusion from this short analysis is that if the heat exchanger design, or the operating conditions show possibilities of static instability effects, this may lead to instable operation. If several solutions for the thermal-hydraulic balance for a heat exchanger can exist, there will always be a chance that “switching” between them in operation may occur due to process disturbances. A temperature profile in a heat exchanger as shown in Figure 7b could be undesirable also when neighboring layers have only moderate temperature differences if the flow rates are alternating between equal and unequal flow distribution during operation.

#### 4. Summary and conclusions

In this work a detailed plate-fin heat exchanger model was developed using a flexible heat exchanger modelling framework. It was designed to be used as the main cryogenic heat exchanger, with three streams, in a single mixed refrigerant process for liquefaction of natural gas. The purpose of the model was to be able to investigate the effects of non-ideal behavior arising from asymmetric layer configuration or from unfortunate operating conditions. When calculating each layer in the heat exchanger individually, it was shown that the effects of various layer stacking pattern may require oversizing of 20 to 40% when compared

to a reference case using a stream-by-stream heat exchanger modelling approach. The model was also used to investigate effects of operating under conditions where static instability might occur. In this situation, two unique solutions for the mass flow distribution were obtained depending on the initial values. Strong thermal coupling through parting sheet ensured small local temperature differences between neighboring layers. However, a total of 100 K temperature difference between the left and right (or back and front) side of a single heat exchanger core was found, which emphasizes that a heat exchanger design or operating condition where multiple solutions of the thermal-hydraulic balance can exist should be avoided.

## Acknowledgments

This publication is based on results from the research project “Enabling low emission LNG systems”, performed under the Petromaks program. The author(s) acknowledge the project partners; Statoil and GDF SUEZ, and the Research Council of Norway (193062/S60) for support. The author(s) also acknowledge the contributions from Harald T. Walnum and Ailo Aasen.

## References

- [1] Aspen Technology, Inc, 2011. Aspen MUSE. Aspen Engineering Suite V7.3.
- [2] Bell, J., Ghaly, M., 1973. An approximate generalized design method for multicomponent/partial condensers. AIChE symp. series, heat transfer: 69 (72-79).
- [3] Bennett, D. L., Chen, J. C., 1980. Forced convective boiling in vertical tubes for saturated pure components and binary mixtures. AIChE Journal 26 (3), 454–461.
- [4] Boyko, L. D., Kruzhilin, G. N., 1967. Heat transfer and hydraulic resistance during condensation of steam in a horizontal tube and in a bundle of tubes. Int. J. Heat Mass Transfer 10, 361–373.
- [5] Chang, H.-M., Lim, H. S., Choe, K. H., 2012. Effect of multi-stream heat exchanger on performance of natural gas liquefaction with mixed refrigerant. Cryogenics 52 (12), 642–647.
- [6] Filonenko, F. K., 1954. Hydraulic resistance in pipes (in russian). Teploenergetika 1 (4), 40–44.
- [7] Fong, K. W., Jefferson, T. H., Suyehiro, T., Walton, L., July 1993. Guide to the SLATEC Common Mathematical Library. [www.netlib.org/guide](http://www.netlib.org/guide).
- [8] Friedel, L., 1979. Improved friction pressure drop correlation for horizontal and vertical two phase pipe flow. In: European Two phase Flow Group Meeting, ISPR. Vol. Paper E-2.
- [9] Gnielinski, V., 1976. New equations for heat and mass transfer in turbulent pipe and channel flow. Int. Chem. Eng. 16 (2), 359–368, GIHA.
- [10] Hesselgreaves, J., 2001. Compact Heat Exchangers: Selection, Design and Operation. Pergamon.
- [11] Ledinegg, 1938. Instabilität der strömung bei natürlichen und zwangsumlauf. Die Wärme 48, 891–898.
- [12] Manglik, R., Bergels, A., 1995. Heat transfer and pressure drop correlations for the rectangular offset strip fin compact heat exchanger. Experimental Thermal and Fluid Science 10 (2), 171–180.
- [13] Reneaume, J., Niclout, N., 2003. Minlp optimization of plate fin heat exchangers. Chemical Biochem. Eng. Q 17 (1), 65–76.
- [14] Reneaume, J. M., Niclout, N., 2001. Plate-fin heat exchanger design using simulated annealing. Vol. 9. Elsevier, Amsterdam, The Netherlands, pp. 481–486.
- [15] Silver, L., 1947. Gas cooling with aqueous condensation. Trans. Inst. Chem. Eng. 25, 30–47.
- [16] Skaugen, G., Gjøvåg, G. A., Nekså, P., Wahl, P. E., 2010. Use of sophisticated heat exchanger simulation models for investigation of possible design and operational pitfalls in lng processes. Journal of Natural Gas Science and Engineering 2 (5), 235–243.
- [17] Skaugen, G., Kolsaker, K., Walnum, H. T., Wilhelmsen, Ø., 2013. A flexible and robust modelling framework for multi-stream heat exchangers. Computers & Chemical Engineering 49 (0), 95–104.
- [18] Wang, M., Zhang, J., Xu, Q., 2012. Optimal design and operation of a C3MR refrigeration system for natural gas liquefaction. Computers & Chemical Engineering 39 (0), 84–95.